



Physical Properties and Fast Neutron Remove Cross Section of PbO-MgO-Bi₂O₃-B₂O₃ Glasses

Hawwa M. Asmaial^{1,4,5}, Zeinab Algadhi^{2,4}, Seham Y. M. Dogharsham^{3,4*},
Hend A. Saltani^{1,4}, Ibrahim M. hammamu^{1,4}, Daefalla M. Tawati^{1,4}

¹ Physics Department, Science Faculty, The University of Benghazi, Benghazi, Libya

² General Department, Science Faculty, The University of Benghazi, Benghazi, Libya

³ Engineering Sciences Department, Engineering Faculty, Ajdabiya University,
Ajdabiya, Libya

⁴ Physics Research Group, Science Faculty, The University of Benghazi, Benghazi, Libya

⁵ Medical Physics Department, Health Ministry, Libyan government, Benghazi, Libya

الخصائص الفيزيائية والمقطع العرضي الفعال لإزالة النيوترونات السريعة لزجاج PbO-MgO-Bi₂O₃-B₂O₃

حواء محمد إسماعيل^{1,4,5}، زينب القاضي^{2,4}، سهام يوسف محمد دقارش^{3,4*}، هند أبوبكر السلطاني^{1,4}،

إبراهيم محمد حممو^{1,4}، ضيف الله محمد التواتي^{1,4}

¹ قسم الفيزياء، كلية العلوم، جامعة بنغازي، بنغازي، ليبيا

² القسم العام، كلية العلوم، جامعة بنغازي، بنغازي، ليبيا

³ قسم العلوم الهندسية، كلية الهندسة، جامعة اجدابيا، اجدابيا، ليبيا

⁴ مجموعة أبحاث الفيزياء، كلية العلوم، جامعة بنغازي، بنغازي، ليبيا

⁵ قسم الفيزياء الطبية، وزارة الصحة، الحكومة الليبية، بنغازي، ليبيا

*Corresponding author: s.yousf2525@gmail.com

Received: September 10, 2025

Accepted: November 20, 2025

Published: December 01, 2025

Abstract:

This study analyzed the physical parameters of xPbO-10MgO-25Bi₂O₃-(65-x) B₂O₃ glasses with x values of 5, 10, 15, 20, 25, and 30 mol%, including density of glass (ρ_g), volume of molar (V_M), molar volume of oxygen (V_O), oxygen packing density (OPD), Poisson's rate (σ), oxygen ions (N_{O-ions}) and lead ions concentration ($N_{Pb-ions}$). As PbO concentration increases in the matrix of glass, the density, volume of molar, molar volume of oxygen, and $N_{Pb-ions}$ increase. Conversely, as the concentration of PbO increases, OPD and N_{O-ions} decrease. The Poisson's rate values suggest a strengthening of the binding within the matrix of glass. Furthermore, to examine the glass material as a shield against fast neutrons, the effective removal cross-section for fast neutrons (FNRCS or $\sum R$) was computed theoretically. Based on the information obtained, it has been reported that the incorporation of lead oxide enhanced the physical properties of the glass samples, which exhibited greater shielding efficiency against fast neutrons compared to various materials.

Keywords: Borate glass, density, volume of molar, Poisson's rate, oxygen ions density, FNRCS.

الملخص

تم دراسة المعايير الفيزيائية للزجاج xPbO-10MgO-25Bi₂O₃-(65-x) B₂O₃ بنسب 5 و 10 و 15 و 20 و 25 و 30 مول %، بما في ذلك كثافة الزجاج (ρ_g) والحجم المولي (V_M) والحجم المولي للأكسجين (V_O) وكثافة تعبئة الأكسجين (OPD) ونسبة بواسون (σ) وتركيز أيونات الأكسجين (N_{O-ions}) و أيونات الرصاص ($N_{Pb-ions}$). تبين أن الكثافة والحجم المولي والحجم المولي للأكسجين و أيونات الرصاص $N_{Pb-ions}$ تزداد بزيادة تركيز أكسيد الرصاص PbO في

مصفوفة الزجاج وبالمقابل، تقل أيونات OPD و NO-ion . تشير قيم نسبة بواسون إلى زيادة الارتباط في مصفوفة الزجاج. كما تم حساب المقطع العرضي الفعال لإزالة النيوترونات السريعة (FNRCS) نظرياً، لبيان فعالية الزجاج كدرع ضد النيوترونات السريعة. وبناءً على النتائج التي تم الحصول عليها، فقد تبين أن دمج أكسيد الرصاص عزز الخصائص الفيزيائية لعينات الزجاج، والتي أظهرت كفاءة حماية أكبر ضد النيوترونات السريعة مقارنة بالمواد المختلفة.

الكلمات المفتاحية: زجاج البورات، الكثافة، الحجم المولاري، نسبة بواسون، كثافة أيونات الأكسجين، FNRCS.

1. Introduction







Today, there is a lot of interest in the production of enhanced, safe substances such as oxide glasses for a variety of uses, particularly in the area of shielding and protecting against nuclear radiation. These materials have gained considerable interest due to their tunable physical properties, chemical durability, and transparency, which are superior to those of traditional shielding materials like lead and concrete [1, 2]. Among the several oxide glasses, boron oxide is a very important glass-forming forming due to its low viscosity, remarkable mechanical and thermal stability [3]. Borate glasses modified with lead and bismuth oxides are garnering increased attention due to their ability to improve physical characteristics and radiation shielding efficacy [1, 4]. Borate glasses' physical characteristics, including density, volume of molar, and packing density, are critical in establishing the glass structure, stability, and, most significantly, neutron attenuation capability [4-6, 7, 8]. The incorporation of heavy metal oxides, including PbO and Bi_2O_3 , is particularly significant due to their high atomic numbers, which enhance the probability of neutron and gamma-ray interactions [9]. Glass containing Bi_2O_3 offers advantageous optical and electrical characteristics, including a high dielectric constant, expanded permeability in the mid-infrared, and a high refractive index [10]. The present work examines the physical properties and fast neutron removal cross sections of $\text{PbO-MgO-Bi}_2\text{O}_3\text{-B}_2\text{O}_3$ glasses to assess their potential for nuclear radiation shielding uses.

2. Material and methods

2.1 Preparing Glass Samples

Six glass samples of the combination $x\text{PbO-10MgO-25Bi}_2\text{O}_3\text{-(x-65) B}_2\text{O}_3$ ($x = 5, 10, 15, 20, 25, 30 \text{ mol\%}$) were made using standard melt quenching techniques. The analytically pure reagents of PbO , MgO , Bi_2O_3 , and H_3BO_3 were taken as raw materials.

Table 1 Photos of the prepared samples

Glass code	Glass composition (mol%)	Prepared glasses
P1	$5\text{PbO-10MgO-25Bi}_2\text{O}_3\text{-60B}_2\text{O}_3$	
P2	$10\text{PbO-10MgO-25Bi}_2\text{O}_3\text{-55B}_2\text{O}_3$	
P3	$15\text{PbO-10MgO-25Bi}_2\text{O}_3\text{-50B}_2\text{O}_3$	
P4	$20\text{PbO-10MgO-25Bi}_2\text{O}_3\text{-45B}_2\text{O}_3$	
P5	$25\text{PbO-10MgO-25Bi}_2\text{O}_3\text{-40B}_2\text{O}_3$	
P6	$30\text{PbO-10MgO-25Bi}_2\text{O}_3\text{-35B}_2\text{O}_3$	

The required quantities of these chemical powders were weighed accurately using a Haus Discovery electronic equilibrium with a precision of 0.1 mg. After that, the mixes were mixed and blended in alumina crucibles, each weighing approximately 19 grams, and put in a 350°C electric furnace for around an hour. This initial heating aimed to promote crosslinking among the compounds and ensure sample homogeneity. Afterward, the furnace temperature was gradually raised to $(900 - 1100^\circ\text{C})$, where it was held for one hour to complete the melting process, with the mixture being stirred frequently to get rid of any bubbles and create a completely homogenous admixture. The melting temperature varied depending on the PbO content. After pouring the melt onto a stainless-steel plate form and annealing it for one hour at 400°C in a preheated stainless-steel mold, it was

slowly cooled to room temperature. The goal of this process is to remove the glass's internal stress and keep it from cracking. The samples of glass have dimensions of around 5 mm thick and 2.5 cm in diameter. The fabricated samples of glass are shown in Table 1.

2.2 Glass density and other related parameters

Archimedes method was applied at room temperature to measure the density of all samples utilizing xylene as a liquid for immersion. An electronic balance with a 1 mg precision was used to weigh the samples. The glass density was calculated using the following formula; ρ_g [3, 8].

$$\rho_g = \frac{W_a}{W_a - W_x} \times \rho_x \quad (1)$$

Where ρ_g and ρ_x are the densities of glass and xylene, respectively ($\rho_x = 0.861 \text{ g.cm}^{-3}$), w_a is the sample weight in air, and w_x is the sample weight in xylene [6, 8].

The volume of molar (V_M) refers to the volume of glass per mole of its constituent atoms or molecules. It is calculated by [1, 6, 11].

$$V_M = \frac{M}{\rho_g} \quad (2)$$

Where M is the mixture's molecular weight.

The molar volume of oxygen (V_O) of each glass sample is obtained using the formula [1, 9]:

$$V_O = \frac{V_M}{\sum x_i n_i} \quad (3)$$

Where x_i represents the mole fraction and n_i represents the number of oxygen atoms for each oxide component, respectively.

The oxygen packing density (OPD), which provides information on how densely the glass network is packed and is crucial to understanding glass structure, can be calculated using the formula below [1, 14]:

$$OPD = 1000C\left(\frac{\rho_g}{M}\right) \quad (4)$$

Here C is the total sum of atoms of oxygen.

The relationship is used to calculate the packing density (V_t) [12, 13]:

$$V_t = \frac{\sum V_i X_i}{V_M} \quad (5)$$

Where the packing density parameter is denoted by V_i , and this parameter for the oxide M_xO_y is given by [9, 14].

$$V_i = \frac{4}{3} \pi N_A (X \cdot r_M^3 + Y \cdot r_O^3) \quad (6)$$

where N_A is Avogadro's number and r_M and r_O are the ionic radii of metal and oxygen, respectively. The numbers of metal and oxygen atoms are denoted by X and Y , respectively.

The packing density (V_t) can be used to determine the Poisson's rate (σ) for the prepared glass samples by using the relation [8, 13]:

$$\sigma = 0.5 - \left(\frac{1}{7.2V_t} \right) \quad (7)$$

The oxygen ions ($N_{O\text{-ions}}$) density and the lead ion ($N_{Pb\text{-ions}}$) density of the studied glasses can be computed by the following equation [8, 14]:

$$N_{O\text{-ions}} = \frac{n_i x_i \rho_g N_A}{M} \quad (8)$$

$$N_{Pb\text{-ions}} = \frac{n_{Pb} x_{PbO} \rho_g N_A}{M_{PbO}} \quad (9)$$

Where N_A is the Avogadro's number.

2.3 Determination of Fast Neutron Removal Cross Section (FNRCs or ΣR)

FNRCs is a crucial parameter used to evaluate the effectiveness of material in shielding against fast neutrons. Unlike gamma rays or X-rays, which are attenuated primarily by photoelectric effect, Compton scattering, and pair production, fast neutrons lose energy mainly through elastic and inelastic scattering with atomic nuclei within the shielding material. ΣR , evaluates a material's efficacy in attenuating neutrons [5, 15]. A higher ΣR value implies a greater ability of the material to reduce neutron penetration and intensity, which is essential for designing effective neutron shielding systems [1, 3, 4]. The ΣR (cm^{-1}) for a compound or a homogeneous mixture is typically obtained by the equations [15]:

$$\Sigma_R(\text{cm}^{-1}) = \sum_i (\rho_g)_i \left(\frac{\Sigma_R}{\rho_g} \right)_i \quad (10)$$

$$(\rho_g)_i = w_i \rho_g \quad (11)$$

Where, $(\rho_g)_i$, $\left(\frac{\Sigma_R}{\rho_g} \right)_i$ and w_i are the partial density, mass removal cross-section of the i th constituent, and weight fraction of the i^{th} elements for each glass samples respectively. $\left(\frac{\Sigma_R}{\rho_g} \right)_i = \Sigma_R$ ($\text{cm}^2 \cdot \text{g}^{-1}$) can be found for any element using equations [12,16].

$$\Sigma_R (\text{cm}^2 \cdot \text{g}^{-1}) = 0.190 Z^{-0.743} \quad Z \leq 8 \quad (12)$$

$$\Sigma_R (\text{cm}^2 \cdot \text{g}^{-1}) = 0.125 Z^{-0.565} \quad Z > 8 \quad (13)$$

Where, Z is the atomic number of an element that shearing in the glass matrix.

3. Results and discussion

3.1. Physical Properties

The physical properties of the present glasses, including ρ_g , VM, V_0 , OPD, σ , NO-ions, and NPb-ions, are computed by equations (1-9) and listed in Table 2. Table 2 and Figure 1 make it evident that the ρ_g is increasing as PbO increases. This increase in density as PbO increases is perhaps due to the higher molecular weight of PbO ($223.2 \text{ g} \cdot \text{mol}^{-1}$) compared to that of B_2O_3 ($69.62 \text{ g} \cdot \text{mol}^{-1}$). Table 2 and Figure 2 show that the ρ_g continuously increases as PbO increases, while the VM values first increase from 33.91 – 34.79 with PbO content (from 5 to 20 mol%) and after that decrease from 34.79 to 34.04 with PbO content (from 20 to 30 mol%). This result demonstrated raising the PbO content in the formulation complexly affects both density and molar volume.

Table 2 Physical Parameters of the glass system $x\text{PbO}-10\text{MgO}-25\text{Bi}_2\text{O}_3-(65-x)\text{B}_2\text{O}_3$.

SN.	Sample Code	P1	P2	P3	P4	P5	P6
1	ρ_g (gcm^{-3})	5.1144	5.3203	5.4641	5.6481	5.9895	6.2231
2	M (g/mol.)	173.45	181.13	188.81	196.49	204.17	211.85
3	V_M ($\text{cm}^3 \text{mol}^{-1}$)	33.91	34.05	34.55	34.79	34.09	34.04
4	V_O ($\text{cm}^3 \text{mol}^{-1}$)	12.56	13.09	13.82	14.50	14.82	15.47
5	OPD (mol L^{-1})	79.61	76.37	72.35	68.99	67.47	64.63
6	σ	0.2692	0.2627	0.2532	0.2452	0.2438	0.2373
7	$N_{O\text{-ions}}$ ($\times 10^{22} \text{ cm}^{-3}$)	9.29	9.05	8.66	8.29	8.10	7.69
8	$N_{Pb\text{-ions}}$ ($\times 10^{21} \text{ cm}^{-3}$)	0.69	1.43	2.21	3.05	4.04	5.05

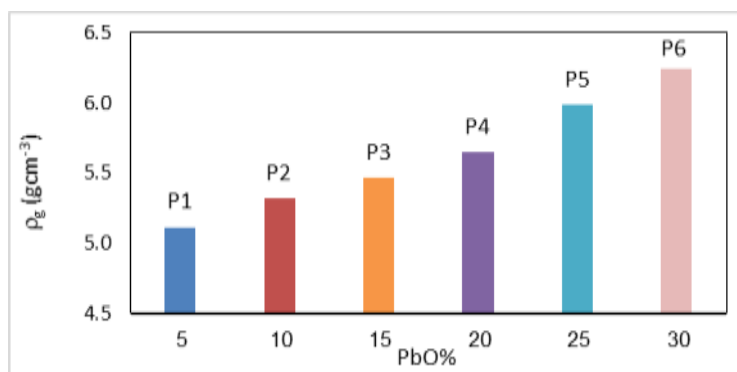


Figure 1: Changes in the ρ_g with PbO mol% content.

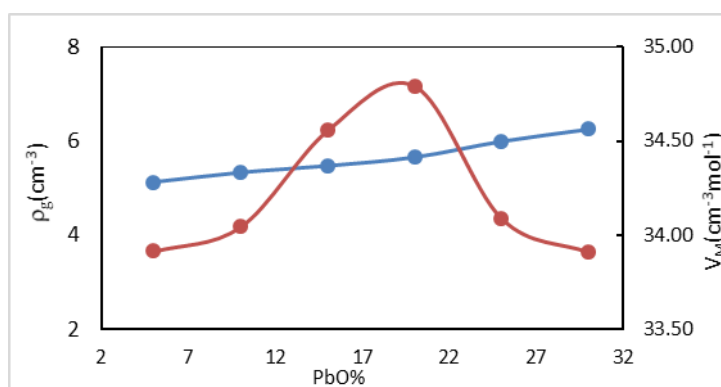


Figure 2: Changes in ρ_g and V_m with PbO mol % content.

This increase in the volume of molar with increasing PbO content in the first stage suggests that the addition of lead oxide results in the incorporation of large lead ions into the glass lattice. Although the lead ions increase the total mass (and thus density), their large ionic size may also lead to greater interatomic spacing, thus increasing the volume of molar. This transformation is made possible by the expansion of the glass network, which indicates that the glass matrix's structure is more open [8]. This could be because PbO produces more non-bridging oxygen in the glass network than B₂O₃. However, the decrease in volume of molar during the second stage, while density continues to increase, indicates a change in the structural role of PbO within the glass lattice at higher concentrations, and this may be attributed to the glass matrix forming a more compact and cross-linked structure [16]. The parameter OPD is a measure of how tightly packed the oxygen ions are within the glass network. It indicates the degree of compactness of the glass structure. In other words, OPD represents the stiffness index of glass samples. As seen in Table 2 and Figure 3, V_O increases with increasing PbO content, while OPD decreases. This suggests that as there are fewer linkages in the matrix, the glass structure gets tighter [9].

The Poisson rate of glassy complexes is often affected by the change in cross-link density brought about by structural alteration [9, 14]. Additionally, σ indicates the stiffness of the glass system; Poisson's rate typically falls between 0 and 0.5 for most materials. Cross-linking density is high in materials with a Poisson's rate less than 0.3 and low in those with a rate greater than 0.3 [11]. The produced glass samples exhibit a high cross-link density, as shown by Table 2 and Figure 4, with Poisson's ratio values falling between 0.2692 and 0.2373. This implies a better cross-link density of the tiled glasses, which is an indication of the best application of shielding performance [14]. Figure 4 shows Poisson's rate (σ) versus molar percentage of PbO. The density of oxygen ions and Poisson's rate decreased from 0.2692 to 0.2373. The inverse behavior of these parameters can be explained by the fact that the density and volume of molar of the glass affect the values of these parameters. The findings show that the addition of PbO alters the oxygen atoms' packing order in the glass lattice, changing the OPD and the molar volume of oxygen. This decreases linearly with an increasing molar percentage of PbO in the samples.

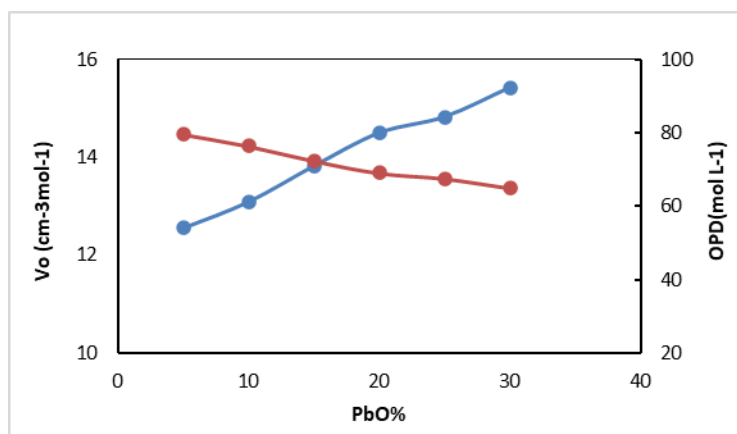


Figure 3: Shows the mole percent of PbO vs. the mole volume of oxygen (VO) and OPD.

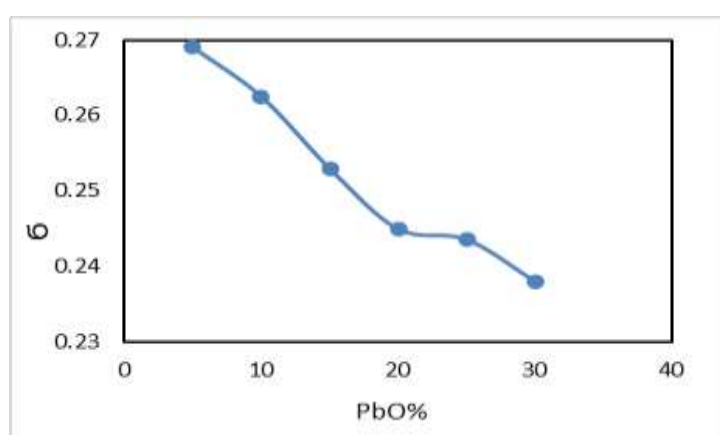


Figure 4: Poisson's ratio (σ) versus the mol percent of PbO.

One of the most important factors in the research of glass structure is the concentration of oxygen ions ($N_{O\text{-ions}}$) in the glass networks. Its impacts a wide range of glass properties, including: Mechanical, Optical, thermal, and other properties. The relation, $N_{O\text{-ions}}$ versus %PbO content is depicted in Figure 5. It has seen that; the $N_{O\text{-ions}}$ decreases from $(9.29 \text{ to } 7.69) \times 10^{22} \text{ ions cm}^{-3}$ as PbO increasing in the glass network. This relationship is due to the structural changes that occur when PbO is incorporated into the glass network. Lead oxide (PbO) often acts as a network modifier in glass structures. This means it disrupts the existing network of glass-forming oxides like B_2O_3 . When PbO is introduced, it can break bonds in the existing network, leading to a decrease in the number of bridging oxygen ions (those shared between two network-forming units) and an increase in non-bridging oxygen ions (those not shared). The heavier lead atoms, combined with the structural changes caused by PbO, lead to a denser glass structure. This is because lead ions can pack more tightly into the spaces created by the broken bonds [17]. The number density of Pb ions ($N_{\text{ions-Pb}}$) for the studied glass samples shows noticeable variation depending on the PbO concentration in the glass composition, with values ranging from 0.69×10^{21} to $5.05 \times 10^{21} \text{ ions cm}^{-3}$. Because lead has a large atomic weight and density, this pattern clearly shows that adding PbO to the glass network considerably raises the ionic concentration. At lower PbO contents, the number density values are relatively small, which reflects a reduced contribution of Pb ions to the overall glass matrix. However, as the PbO ratio increases, a progressive enhancement in $N_{\text{Pb-ions}}$ is observed, with the maximum value of $5.05 \times 10^{21} \text{ ions cm}^{-3}$ corresponding to the glass sample containing the highest PbO fraction.

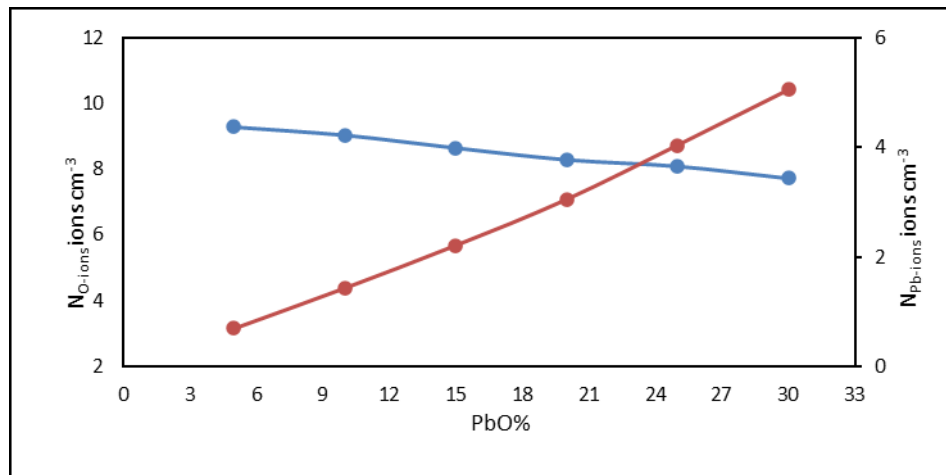


Figure 5: Shows the density of oxygen ions (N_{O-ions}) and lead ions ($N_{Pb-ions}$) in relation to the mol % of PbO.

3.2 Fast Neutron Removal Cross Section (FNRCS)

Figure 6 illustrates the fast neutron removal cross section (ΣR , cm^{-1}) values for the synthesized glass samples, which were computed based on the weight fractions of the constituent elements and the corresponding sample densities using equations (12) and (13). Table 3 shows the removal cross-section calculation process in detail as well as the cross-section values that were achieved for each glass sample. The estimated results showed that the P4 glass with (PbO = 20% and B₂O₃ = 45%) possesses the lowest FNRCS ($\Sigma R = 0.1072 \text{ cm}^{-1}$), while P1 with (PbO = 5% and B₂O₃ = 60%) possesses the highest FNRCS ($\Sigma R = 0.1115 \text{ cm}^{-1}$).

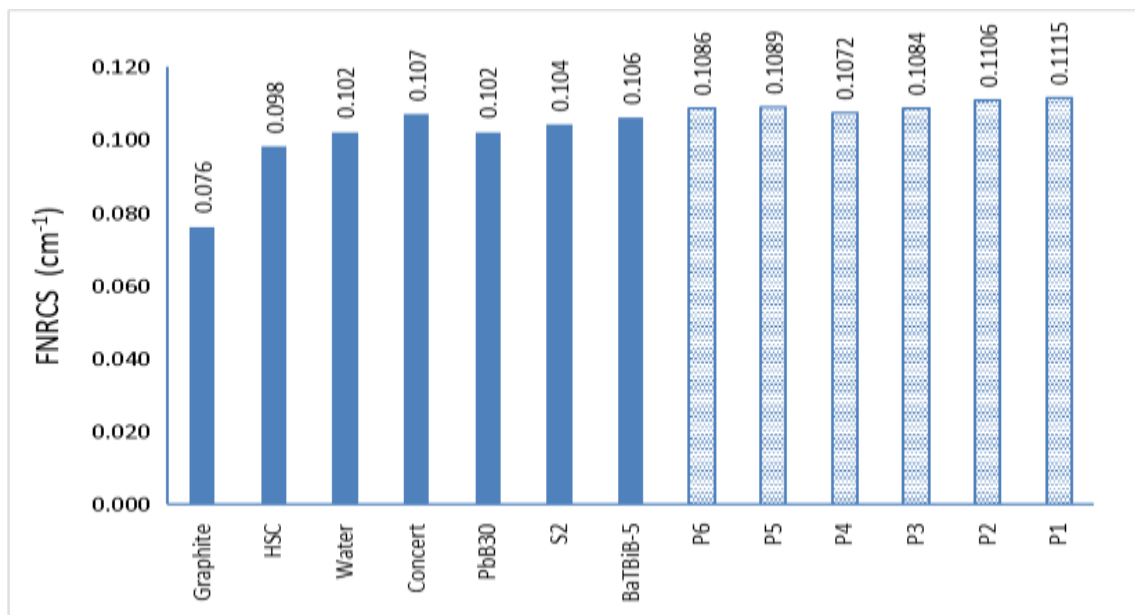


Figure 6: Fast Neutron removal cross section of prepared glass samples and standard neutron shielding materials. Patterned columns indicate present work.

Table 3 Partial density and Fast Neutron Removal Cross Section of PbO-MgO-Bi₂O₃-B₂O₃ glasses.

Sample: P1				
Element	$\Sigma R/\rho_g$ (cm ² .g ⁻¹)	w. f.e (%)	partial density (g.cm ⁻³)	ΣR (cm ⁻¹)
Pb	0.0106	0.0597	0.3055	0.0032
O	0.0405	0.2491	1.2740	0.0516
Mg	0.0311	0.0140	0.0717	0.0022
Bi	0.0105	0.6024	3.0810	0.0324
B	0.0575	0.0748	0.3825	0.0220
Total cross-section				0.1115

Sample: P2				
Element	$\Sigma R/\rho$ (cm ² .g ⁻¹)	w. f.e (%)	partial density (g.cm ⁻³)	ΣR (cm ⁻¹)
Pb	0.01060	0.1144	0.6086	0.0064
O	0.04053	0.2297	1.2219	0.0495
Mg	0.03109	0.0134	0.0714	0.0022
Bi	0.01053	0.5769	3.0692	0.0323
B	0.05747	0.0657	0.3493	0.0201
Total cross-section				0.1106

Sample: P3				
Element	$\Sigma R/\rho$ (cm ² .g ⁻¹)	w. f.e (%)	partial d (g.cm ⁻³)	ΣR (cm ⁻¹)
Pb	0.0106	0.1646	0.8994	0.0095
O	0.0405	0.2118	1.1575	0.0469
Mg	0.0311	0.0129	0.0703	0.0022
Bi	0.0105	0.5534	3.0239	0.0318
B	0.0575	0.0573	0.3129	0.0180
Total cross-section				0.1084

Sample: P4				
Element	$\Sigma R/\rho$ (cm ² .g ⁻¹)	w. f.e (%)	partial d (g.cm ⁻³)	ΣR (cm ⁻¹)
Pb	0.01060	0.2109	1.19120	0.0126
O	0.04053	0.1954	1.10377	0.0447
Mg	0.03109	0.0124	0.06986	0.0022
Bi	0.01053	0.5318	3.00358	0.0316
B	0.05747	0.0495	0.27969	0.0161
Total cross-section				0.1072

Sample: P5				
Element	$\Sigma R/\rho$ (cm ² .g ⁻¹)	w. f.e (%)	partial d (g.cm ⁻³)	ΣR (cm ⁻¹)
Pb	0.0106	0.2537	1.5196	0.0161
O	0.0405	0.1802	1.0795	0.0438
Mg	0.0311	0.0119	0.0713	0.0022
Bi	0.0105	0.5118	3.0653	0.0323
B	0.0575	0.0424	0.2537	0.0146
Total cross-section				0.1089

Sample: P6				
Element	$\Sigma R/\rho$ (cm ² .g ⁻¹)	w. f.e (%)	partial d (g.cm ⁻³)	ΣR (cm ⁻¹)
Pb	0.0106	0.2934	1.8260	0.0193
O	0.0405	0.1662	1.0340	0.0419
Mg	0.0311	0.0115	0.0714	0.0022
Bi	0.0105	0.4932	3.0694	0.0323
B	0.0575	0.0357	0.2223	0.0128
Total cross-section				0.1086

The reason why P1 glass has the highest FNRCS is might be due to that P1 contained the highest content of Boron over all the prepared glasses, making it a good neutron absorber. [18, 19].

Additionally, Figure 6 displays a comparison of the removal cross-sections of the constructed glasses with additional neutron-shielding substances discovered in the literature [8, 18, 19, 20]. It's clear that the developed glass samples demonstrate higher removal cross section values compared to materials such as graphite, hematite-serpentine concrete (HSH), water and other glasses like: Pb30(30PbO-10WO₃-10Na₂O-10MgO-40B₂O₃), S2(10Al₂O₃-10Bi₂O₃-10Na₂O₃-70B₂O₃) and BaTBiB-5(25BaO-5TeO₂-35Bi₂O₃-35B₂O₃). These results make the current glass potentially usable in many applications, especially in radiation protection.

4. Conclusion

The physical characteristics and FNRCS for different compositions of PbO-MgO-Bi₂O₃-B₂O₃ were investigated. The results demonstrated that an increase in density and volume of molar coincided with an increase in PbO, with PbO content (5–20 mol%) and then decreased with PbO content (20–30 mol%). This is suggesting that in first stage, a potential expansion of the glass network and a more open glass structure inside the glass matrix. In the second stage, the network structure of the glass becomes more condensed and interconnected. The oxygen packing density (OPD) and molar volume of oxygen (V_O) responded paradoxically; a drop in OPD was seen to counteract an increase in V_O. According to this, the glass structure gets more compact as the matrix's bond count drops. The Poisson's rate readings indicate a tightening of the bonds within the glass matrix. The decrease in oxygen ion concentration with increasing lead oxide and increasing glass density results in a significant increase in mass per unit volume. In addition, while increasing the number density of lead ions (N_{Pb-ions}), lead ions, being larger in size, can efficiently fill the glass networks' interstitial spaces, increasing the packing tightness without a proportional increase in overall volume. Additionally, it was demonstrated that by raising the FNRCS in comparison to a number of other materials, the addition of PbO improved the glass's capacity to screen fast neutrons.

Comprehensively, the results showed that PbO addition enhanced the glass samples' FNRCs and their physical characteristics, enabling their usage in a variety of applications, including shielding of radiation.

5. Acknowledgement

We would like to thank everyone who helped us finish this study by offering their advice and guidance. Special thanks to Dr. Ali Al-Shooly, Dean of the Faculty of Electrical and Electronics Technology, Benghazi, Libya, for allowing us access to a laboratory to conduct this research.

Compliance with ethical standards

Disclosure of conflict of interest

The authors declare that they have no conflict of interest.

6. References

- [1] E. M. Çelikkilek, A. E. Ersundu, N. Gedikoğlu, E. Şakar, M. Büyükyıldız, and M. Kurudirek, "Physical, mechanical and gamma-ray shielding properties of highly transparent ZnO-MoO₃-TeO₂ glasses," J. Non-Cryst. Solids, 2019, Vol. 524, pp. 119648.
- [2] M. H. M. Zaid, H. A. A. Sidek, K. A. Matori, A. Abdu, K. A. Mahmoud, M. M. Al-Shammari and M. I. Sayyed, "Influence of heavy metal oxides to the mechanical and radiation shielding properties of borate and silica glass system," J. Mater. Res. Technol, 2021, Vol. 11, pp. 1322-1330
- [3] A. Kumar, R. Kaur, M.I. Sayyed, M. Rashad, M. Singh and A.M. Ali, "Physical, structural, optical and gamma ray shielding behavior of (20+x)PbO–10BaO–10NaO–10MgO–(50-x)BO glasses", Phys. B Condensed Matter, 2018, Vol. 552, pp. 110-118
- [4] H. Al-Ghamdi, M.I. Sayyed, A. Kumar, S. Yasmin, B.O. Elbashir and A.H. AL Muqrin, "Effect of PbO and B₂O₃ on the Physical, Structural, and Radiation Shielding Properties of PbO-TeO₂-MgO-Na₂O-B₂O₃ Glasses," Sustainability, 2022, Vol. 14, pp. 9695
- [5] A. Kumar, M. I. Sayyed, M. Dong, and X. Xue, "Effect of PbO on the shielding behavior of ZnO–P₂O₅ glass system using Monte Carlo simulation," J. Non-Cryst. Solids, 2018, Vol. 481, pp. 604-607
- [6] D. A. Aloraini, A. Kumar, A. H. Almuqrin, and M. I. Abualsayed, "An exploration of the physical, optical, mechanical, and radiation shielding properties of PbO–MgO–ZnO–B₂O₃ glasses," Open Chem., 2023, Vol. 21, pp. 104
- [7] M. Y. Hanfı, M. I. Sayyed, E. Lacomme, I. Akkurt, and K. A. Mahmoud, "The influence of MgO on the radiation protection and mechanical properties of tellurite glasses," Nucl. Eng. Tech. 2021, Vol. 53, pp. 2000–2010.
- [8] S. Singh, R. Kaur, S. Rani and B. S. Sidhu, "Investigations on physical, structural, and nuclear radiation shielding behaviour of niobum-bismuth-cadmium-zinc borate glass system," Prog. Nucl. Energy, 2021, 142, 104038
- [9] A.S. Mater, S.A. Abdelrahman, D. M. Tawati, F. A. Ikraiam, N. A. Hussein and S.S. Basil, "Physical Properties of Bi₂O₃–PbO–P₂O₅ Glasses," AlQalam J. Med. Appl. Sci., 2023, Vol. 7, pp. 1-11
- [10] A. H. Alomari, "Enhancing radiation shielding effectiveness: a comparative study of barium-doped tellurite glasses for gamma and neutron radiation protection," J. Taibah Univ. Science, 2024, 18:1, 2328370
- [11] P. Kaur, K. J. Singh, S. Thakur, P. Singh and B. S. Bajwa, "Investigation of bismuth borate glass system modified with barium for structural and gamma-ray shielding properties," Spectrochimica Acta (A) Molecular and Biomolecular Spectroscopy 2018, Vol. 206, pp. 367–377
- [12] S. Y. M. Dogharsham, O. M. Mailoud, A.A. S. Mater, D. M. Tawati and F. A. Ikraiam, "Mechanical Properties of Ternary Bi₂O₃–PbO–P₂O₅ Glasses," Libyan Journal of Engineering Science and Technology, 2024, Vol. 4, No. 2, pp. 119 – 122.
- [13] S. A. M. Iss, A. Kumar, M. I. Sayyed, M. Dong and Y. Elmahroug, "Mechanical and gamma-ray shielding properties of TeO₂-ZnO-NiO glasses," Material Chemistry and Physics, 2018, Vol. 212, pp. 12-20
- [14] M. I. Sayyed, A. H. Almuqrin, A. Kumar, J.F.M. Jecong and I. Akkurt, "Optical, mechanical properties of TeO₂-CdO-PbO-B₂O₃ glass systems and radiation shielding investigation using EPICS2017 library," Optik, 2021, Vol. 242, 167342
- [15] A. Acikgoz, M. W. Aladailah, O. L. Tashilykov, G. Demircan, M. Kamislioglu, M. M. Yasar, H. Ozdogan and N. Yorulmaz, "Influence of Nd₂O₃ on radiation shielding and elastic properties of TeO₂ – MgO – Na₂O glasses: A simulation Study by PHITS and MCNP," Pramana – J. Phys., 2023, Vol. 97, No. 167, pp. 1-13

- [16] B. O. El-bashir, M. I. Sayyed, M. H. M. Zaid and K. A. Matori, "Comprehensive study on physical, elastic and shielding properties of ternary BaO-Bi₂O₃-P₂O₅ glasses as a potent radiation shielding material," *J. Non-Cryst. Solids*, 2017, Vol. 468, pp. 92-99
- [17] M. I. Sayyed, M. H. A. Mhareb, K. M. Kaky and M. Kh. Hamad, "Structural, Mechanical, and Radiation Shielding Properties of B₂O₃-Na₂O-PbO-Fe₂O₃ glass system," *Radiation Physics and Chemistry*, 2024, Vol. 8, pp. 222, 111848
- [18] S. A. Abdelrahman, R. A. Mansouri, S. Y. M. Dogharsham, A. A. M. Adam and N. A. Hussein, "The Prospective use of Locally produced Borate Glass as Windows and Shields in Imaging Photon and Neutron Environments," *AlQalam J. Med. Appl. Sci.*, 2023, Vol. 7, pp. 1-11
- [19] A. H. Almuqrin, B. Albarzan, O. I. Olarinoye, A. Kumar, N. Alwada and M. I. Sayyed, "Mechanical and Gamma Ray Absorption Behavior of PbO-WO₃-Na₂O-MgO-B₂O₃ Glasses in the Low Energy Range," *Materials*, 2021, Vol. 14, pp. 3466
- [20] A. H. Alomari, "Enhancing radiation shielding effectiveness: a comparative study of barium-doped tellurite glasses for gamma and neutron radiation protection," *J. Taibah Univ. sci*, 2024, Vol. 18, No. 1, 2328370

Disclaimer/Publisher's Note: The statements, opinions, and data contained in all publications are solely those of the individual author(s) and contributor(s) and not of **AJAPAS** and/or the editor(s). **AJAPAS** and/or the editor(s) disclaim responsibility for any injury to people or property resulting from any ideas, methods, instructions, or products referred to in the content.